# A Study of Interstitial Liquid Flow in Foam

RALPH A. LEONARD and ROBERT LEMLICH
University of Cincinnati, Cincinnati, Ohio

## Part I. Theoretical Model and Application to Foam Fractionation

**A theoretical model for interstitial liquid flow in a stationary or moving foam was devised by relating the physical structure of the foam to the physical properties of the surfactant and the foam movement. This was accomplished through a differential momentum balance within a typical capillary (Plateau border) of noncircular cross section with finite surface viscosity at its boundaries. Velocity profiles were then calculated and integrated numerically for the randomly oriented capillaries so as to obtain the overall liquid flow through the foam in terms of the pertinent variables. Results are presented in a form suitable for estimating concentrations and flow rates of product and waste streams in foam fractionation.**

In recent years there has appeared a revival of interest in the potentialities of separating mixtures by foam fractionation. This technique of separation is based on the adsorption of a solute at the surface of bubbles formed by sparging a liquid mixture. These bubbles rise to form a foam which carries solute off overhead. A foam fractionation column can be operated as a refluxing enricher (*16*), a stripper (*17*), or both (*11*). Applications include water renovation (*13, 15*), radioactive effluent purification (*6, 26*), and protein separation (*25*). An extensive review of the literature has recently appeared (*24*).

Some introductory analyses have been presented for the operation of foam fractionation columns (*5, 24*). These analyses show the quantitative role played by surface adsorption. However, they are incomplete in that they do not provide an independent relationship for foam density or for the flow rate of foam overhead. This lack, of course, stems from the complicated nature of foam drainage, especially in a moving column of foam which is constantly being formed at one end and removed at the other.

Accordingly, the present investigation was aimed at devising and testing a more complete model which would include the interstitial liquid flow in the foam. The theoretical development is presented here, together with a design procedure. Experimental confirmation is presented in Part II of this paper. Part II also includes the complete notation for both Parts I and II.

Figure 1 shows a typical foam fractionation column (in this case without external reflux) operating under steady state conditions. By overall balance

$$F = D + W \tag{1}$$

Also, by material balance for a single surfactant

$$C_F F = C_D D + C_W W \tag{2}$$

The surfactant passing overhead, namely $C_D D$, can be divided into two parts so as to represent the physical picture more closely (*5*). The first part is the surfactant adsorbed at the bubble surfaces. This amounts to $6G\Gamma/d_{32}$. The second part is that in the interstitial liquid $C_L D$. Substitution in Equation (2) yields

$$C_F F = C_L D + \frac{6G}{d_{32}}\Gamma + C_W W \tag{3}$$

In a typical situation, $F$, $G$, and $C_F$ might be the given independent variables. Average bubble diameter $d_{32}$ would depend on $G$, $C_W$, and the sparger. With the feed inlet several diameters or more above the liquid pool, the rising foam would be well rinsed with downcoming feed so that $C_L$ should closely approach $C_F$ if there is no coalescence [breakage] of bubbles in the foam within the column. This pinch in concentration occurs at the level of the feed rather than at the bottom because in the column section below the feed point the rate of liquid downflow exceeds the rate of upflow.

$\Gamma$ can be measured independently in a standard recirculating separator (*5*) or, in certain cases, estimated from surface tension measurements via the Gibbs adsorption equation (*7, 22*). It is fairly constant over a wide range of concentration.

All this effectively leaves the two Equations (1) and (3) with three unknown variables, namely $C_W$, $W$, and $D$. The present study involves the development of a theory for foam drainage which can be used to predict $D$ independently of Equations (1) and (3), thus permitting a more complete solution to the entire problem of foam fractionation.

### FOAM STRUCTURE

Foams can be divided into two extreme types (*1, 19*). These are wet* foams, or kugelschaums, with spherical bubbles and dry† foams, or polyederschaums, with polyhedral bubbles. Except for very small bubble sizes or very viscous liquids, kugelschaums do not normally exist at distances higher than one bubble diameter above the liquid pool. Thus, polyederschaums represent the more usual situation and so will be considered here as forming the basic foam structure.

For a polyederschaum of reasonably uniform bubble size, the foam structure can be approximated by bubbles in the shape of regular dodecahedra (*1, 2, 19*). The bubbles are packed so that their pentagonal faces fit together symmetrically three at a time to form a line, with a dihedral angle of approximately 120 deg. between faces. These lines, in turn, fit together symmetrically four at a time with an angle of approximately 109 deg. between lines.

Of course the packing fit is not perfect. With identical regular dodecahedra, geometric considerations show that

Ralph A. Leonard is with the E. I. du Pont de Nemours and Company, Inc., Wilmington, Delaware.

* Meaning high liquid content.

† Meaning low liquid content.

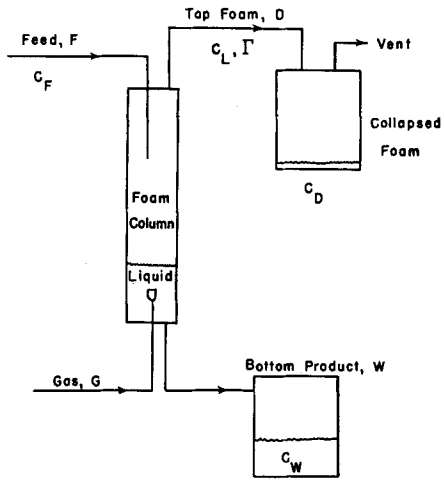


Fig. 1. A typical foam fractionation column.

3% of the space remains unfilled. This contributes to some distortion. However, the picture is fairly good and accordingly is used in the model developed here.

The "unfilled" space between bubbles is actually filled with the interstitial liquid. Most of the liquid is in the aforementioned lines which are really capillaries known as Plateau borders (2). The remaining liquid is in the films that make up the bubble faces.

Figure 2 shows a Plateau border (abbreviated hereafter as PB) in cross section. The shaded area is in sixfold symmetry within a PB.

Flow through a PB is essentially axial. Thus there is little pressure gradient within the PB in the radial or angular directions. Therefore, the pressure difference across the curved PB-gas boundary such as DWE should be virtually uniform from point to point along the boundary. This pressure difference between the liquid in the PB and the gas in the bubble proper is given by the equation of Laplace and Young (1) as

$$p_{out} - p_{in} = \frac{\gamma}{r_o} \tag{4}$$

Since $\gamma$ is uniform, $r_o$ is uniform. Accordingly, boundary DWE is represented as a circular arc. It should be noted that $r_o$ is the radius of curvature of the PB-gas boundary and not the radius of the bubble.

Since each bubble face is essentially flat, there is virtually no corresponding pressure difference between the liquid in a film and the gas in the bubble. Therefore, there must be a sharp pressure gradient within the liquid at the PB-film border, such as at point A of Figure 2. The existence of this sharp gradient has been defended and used to explain marginal regeneration (21).

From geometric considerations

$$A_{PB} = \left(3\sqrt{3} - \frac{3}{2}\pi\right)a^2 + 3at + \frac{\sqrt{3}}{4}t^2 \tag{5}$$

Since $a >> t$ normally, and $r_o = a\sqrt{3}$, Equation (5) reduces to Equation (6):

$$A_{PB} = 0.1612\ r_o^2 + 1.732\ r_o t \tag{6}$$

Also by geometry, Equation (7) gives the packing factor $P$ which is the total length of PBs per unit height of column, and Equation (8) gives the liquid to gas ratio in the foam:

$$P = \frac{60A_{col}}{2.445\ \pi d_{31}^2(1 + V_L/V_G)} \tag{7}$$

$$\frac{V_L}{V_G} = \frac{60A_{PB}}{2.445\pi d_{31}^2} + \frac{3t}{d_{32}} \tag{8}$$

The volumetric density of the foam, $\mathcal{D} = 1 - \epsilon$, is

$$\mathcal{D} = \frac{V_L/V_G}{1 + V_L/V_G} \tag{9}$$

The orientation of a PB in space, without regard to the particular bubble with which it is associated, is taken as being random. This follows from the large number of bubbles present in the foam and the absence of any known factor which would favor one orientation over another.

Foam drainage occurs primarily through the interconnecting PB network (19). In other words, each film drains into its own bounding PBs and, at steady state, does not transmit the drainage of other films (21).

The liquid-gas boundaries, such as *FDWEG* of Figure 2*b*, exhibit a resistance to shear quite apart from that associated directly with the viscosity of the interstitial liquid. The corresponding physical property for this phenomenon has been termed *surface viscosity*. It is defined as the shearing force per unit length in the surface, divided by the resulting velocity gradient in the surface. This can be compared with the familiar bulk viscosity which of course is the shearing force per unit surface within the bulk divided by the velocity gradient in the bulk.

Surface viscosity is attributed to the surfactant which concentrates at the interface (1, 8). It is known to affect drainage (8, 22).

It appears that earlier theoretical models for foam drainage are limited in three ways by their simplifying hypotheses of interstitial flow through channels that are vertical, with rigid walls, and of either substantially circular (10, 20) or parallel plane (4, 9, 14, 23) cross section.

## FLOW THROUGH AN INDIVIDUAL PLATEAU BORDER

In view of the sixfold symmetry of the PB cross section as illustrated in Figure 2*b*, a solution need be obtained only for the shaded region *ADWO* in order to provide a complete velocity profile for flow through a PB. This shaded region is conveniently bounded by cylindrical coordinates about point $P$ as origin, except for the line $AO$ across which mirror symmetry applies.

The equation of motion in cylindrical form (3) for a Newtonian fluid with constant $\rho$ and $\mu$ flowing in the axial

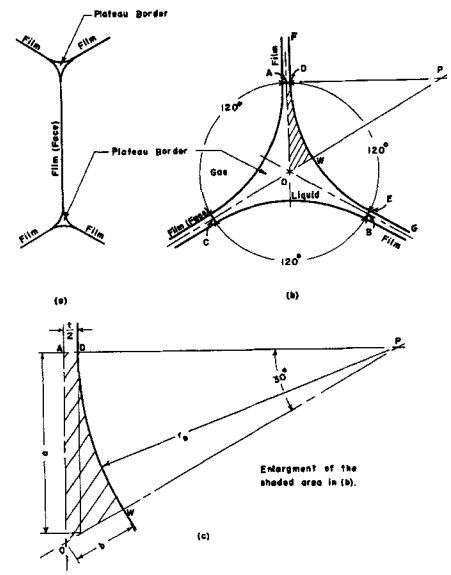


Fig. 2. A Plateau border shown in cross section.

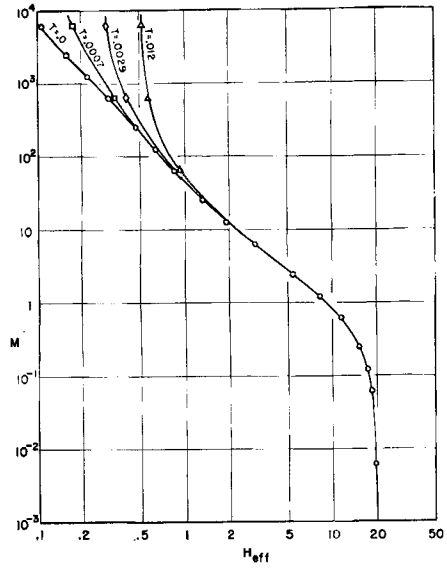


Fig. 3. Dimensionless relationship for flow through a Plateau border.

$z$ direction is

$$\rho\left[\frac{\partial v_z}{\partial \tau}+v_r\frac{\partial v_z}{\partial r}+\frac{v_\theta}{r}\frac{\partial v_z}{\partial \theta}+v_z\frac{\partial v_z}{\partial z}\right]=\frac{-\partial p_{in}}{\partial z}+$$

$$\mu\left[\frac{1}{r}\frac{\partial}{\partial r}\left(r\frac{\partial v_z}{\partial r}\right)+\frac{1}{r^2}\frac{\partial^2 v_z}{\partial \theta^2}+\frac{\partial^2 v_z}{\partial z^2}\right]+\rho g_z \quad (10)$$

It can be shown that $\partial v_z/\partial \tau$, $v_r$, $v_\theta$, $\partial v_z/\partial z$, and $\partial^2 v_z/\partial z^2$ are negligible, and $\partial p_{in}/\partial z << \rho g_z$ so that the quantity $(\rho g_z - \partial p_{in}/\partial z)$ is essentially constant for a given $z$ orientation relative to the earth. Details of this and other aspects of the entire investigation have been placed on file (*17*).

The terms $g_{eff}$ and $h_{eff}$ are now introduced and defined by Equations (11) and (12):

$$g_{eff}=g_z-\frac{1}{\rho}\frac{\partial p_{in}}{\partial z} \quad (11)$$

$$h_{eff}=\frac{\rho g_{eff}}{\mu} \quad (12)$$

Combining with the above one gets

$$\frac{1}{r}\frac{\partial}{\partial r}\left(r\frac{\partial v_z}{\partial r}\right)+\frac{1}{r^2}\frac{\partial^2 v_z}{\partial \theta^2}=-h_{eff} \quad (13)$$

where $h_{eff}$ is constant.

The solution to Equation (13) was obtained through a finite difference approach with fifty-three nodal points. This yielded a matric equation which in turn was solved by means of Crout's reduction (*12*) on an IBM-1620 digital computer. The boundary conditions are those of mirror symmetry at line $OW$ of Figure 2 and mirror symmetry at line $OA$. At the PB-gas interface, namely curve $DW$, the boundary condition is that of momentum transfer to a surface with Newtonian surface viscosity $\mu_s$. This gives $\frac{\partial^2 v_z}{\partial \theta^2}=\frac{-\mu r_o^2}{\mu_s}\frac{\partial v_z}{\partial r}$ at the interface. Elements of this boundary surface move perpendicularly to the PB cross section. For reasons discussed later, point $A$ is conveniently selected as the datum so that $v_z$ at that point is zero.

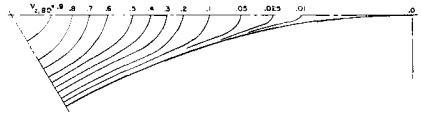

Fig. 4. Lines of constant dimensionless velocity for flow through a Plateau border bounded by rigid interfaces. M = 0 and T = 0.

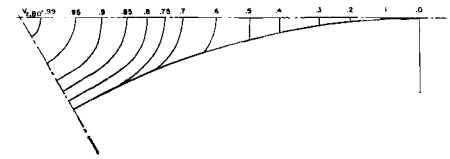

Fig. 5. Lines of constant dimensionless velocity for flow through a Plateau border bounded by interfaces of a moderate surface viscosity. M = 2.48 and T = 0.

The solution for the velocity profile is presented in terms of dimensionless groups defined as follows:

$$H_{eff}=\frac{h_{eff}A_{PB}}{v_{z,\,max}} \quad (14)$$

$$V_z=\frac{v_z}{v_{z,\,max}} \quad (15)$$

$$M=\frac{\mu r_o}{\mu_s} \quad (16)$$

$$T=\frac{t}{r_o} \quad (17)$$

$H_{eff}$ is a function of $M$ and at high $M$ values is also a function of $T$. This is shown in Figure 3.* $V_z$ is a function of $M$ and location in the PB, and also a weak function of $T$. Figures 4, 5, and 6 show lines of constant velocity in a PB cross section for three different cases. In Figure 4 the surface viscosity is very high relative to $\mu r_o$ so that $M = 0$ and the bounding surfaces are rigid.† In Figure 5 the surface viscosity contributes about equally with $\mu r_o$ in determining the flow pattern. In Figure 6 $M$ is large, which means the surface viscosity is low relative to $\mu r_o$, and so $\mu_s$ is the major factor in determining the flow pattern.

Of course, these profiles are restricted to laminar flow. However the experimental results show that flow in the PBs is well within the laminar regime.

PB end effects are neglected, since the PB is relatively long and thin; that is, the ratio $E/a$ is large.

By means of the computer, the velocity profiles were integrated numerically over the cross-sectional area of a PB to yield the volumetric flow rates through an individual PB for various conditions.

In practice $p_{in}$ cannot be easily measured since it is within a PB. This difficulty can be circumvented by differentiating Equation (4) with respect to $z$ and by com-

* The points shown in Figures 3, 8, 9, and 10 are the individual values which were computed from theory in order to establish the curves.

† This case is of special interest quite apart from the present study in foam, as it is identical with the situation for longitudinal laminar flow along (between) close-packed rigid cylinders (*18*).

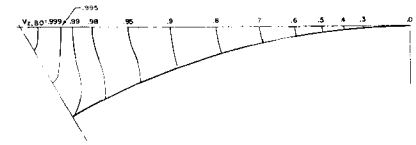

Fig. 6. Lines of constant dimensionless velocity for flow through a Plateau border bounded by interfaces of a very low surface viscosity. M = 61.9 and T = 0.

bining with Equation (11) to give Equation (18):

$$g_{eff} = g_z - \frac{1}{\rho}\frac{dp_{out}}{dz} - \frac{\gamma}{\rho r_o^2}\frac{dr_o}{dz} \qquad (18)$$

In all of the foregoing, velocities are relative to an observer located at the PB-film border such as at point A of Figure 2. Experimental evidence was obtained which indicates that this border observer (designated BO) moves upward relative to an external stationary observer (designated SO) at the same velocity as a moving observer (designated MO) located at the center of a bubble. In other words, evidence indicates that the PB-film border does not move relative to the rising bubbles. However, for the sake of greater generality in derivation, $v_{b,MO} \neq 0$ is allowed in the equations to follow, even though $v_{b,MO} = 0$ will actually be employed in final application.

## OVERALL FLOW

The velocity profiles developed in the previous section are for an individual PB in some particular orientation. Those intermediate results will now be used to obtain an overall picture of the flow of liquid through a foam.

Consider a horizontal plane cutting through a vertical foam column of cross-sectional area $A_{col}$, exposing cross sectional areas totaling $A_h$ in all PBs cut. Since the probable number of intercepted PBs oriented at $\theta$ is $P \sin\theta \cos\theta\, d\theta$, the net rate of volumetric flow upward relative to a stationary observer can be expressed by Equation (19) in terms of the local linear velocities upward through the cutting plane:

$$q_{net\ up,\,SO} = \int_{A_{PB}} \int_0^{\pi/2} v_{up,\,SO} P \sin\theta \cos\theta d\theta\, dA_h \qquad (19)$$

But $dA = \sin\theta\, dA_h$. Furthermore $P$ is constant. Substitution in Equation (19) yields

$$q_{net\ up,\,SO} = P \int_0^{\pi/2} \int_{A_{PB}} v_{up,\,SO}\, dA \cos\theta d\theta \qquad (20)$$

Now consider $v_{z,BO}$ and $v_{b,MO}$ for a vertical PB. Then for a PB inclined at angle $\theta$ from the horizontal, the corresponding velocities are $v_{z,BO}\sin\theta$ and $v_{b,MO}\sin\theta$. Thus the component balance within such an inclined PB is

$$v_{up,\,SO} = v_{f,\,SO} - v_{z,BO}\sin^2\theta - v_{b,MO}\sin^2\theta \qquad (21)$$

as can be seen from Figure 7.*

In the above derivation it is implied that $r_o$ is uniform for a horizontal cross section through the column, which is certainly reasonable. Were it otherwise, liquid would quickly flow from the thicker PBs to the thinner PBs by virtue of Equation (4) until all were of equal $r_o$.

Also implied is that the bulk foam rises through the column in plug flow. This is generally the case and is due in part to the inherent rigidity of the bulk foam. However physical obstacles or severely destructive foam breakage in the column can modify the usual configuration of plug flow.

Equations (22) to (27) define dimensionless groups where $v_{z,max,BO}$, $v_{z,BO}$, and $v_{b,MO}$ refer to a vertical PB. These three velocities thus serve as reference quantities independent of actual PB orientation:

$$Q_{net\ up,\,SO} = \frac{q_{net\ up,\,SO}}{P\, A_{PB}\, v_{z,\,max,\,BO}} \qquad (22)$$

*An important internal check of consistency is that the model predicts local material balance around any intersection of Plateau borders. It can be shown that this follows, regardless of orientation, from the symmetry of the four-way intersection and the proportionality of individual PB flow to $\sin\theta$.

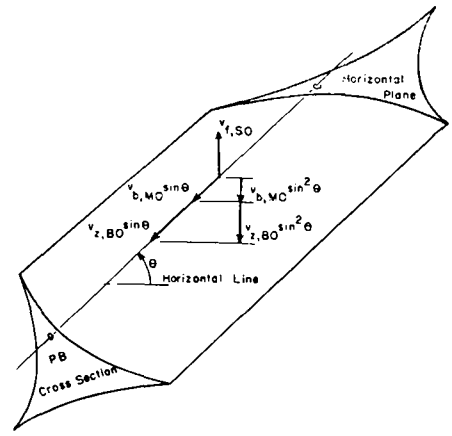


Fig. 7. Velocity components in a Plateau border.

$$dA^+ = \frac{dA}{A_{PB}} \qquad (23)$$

$$V_{up,\,SO} = \frac{v_{up,\,SO}}{v_{z,\,max,\,BO}} \qquad (24)$$

$$V_{f,\,SO} = \frac{v_{f,\,SO}}{v_{z,\,max,\,BO}} \qquad (25)$$

$$V_{z,\,BO} = \frac{v_{z,\,BO}}{v_{z,\,max,\,BO}} \qquad (26)$$

$$V_{b,\,MO} = \frac{v_{b,\,MO}}{v_{z,\,max,\,BO}} \qquad (27)$$

Equations (22) to (27) are then substituted into Equations (20) and (21) which in turn are combined with each other. Analytical integration is then performed term by term to the extent feasible. This yields

$$Q_{net\ up,SO} = V_{f,SO} - \frac{V_{b,MO}}{3} + Q^\circ_{net\ up,SO} \qquad (28)$$

where

$$Q^\circ_{net\ up,SO} = -\int_0^{\pi/2} \int_{A^+_{PB}} V_{z,BO}\sin^2\theta\cos\theta d\theta dA^+ \qquad (29)$$

Equation (30) is a useful alternative form of Equation (28):

$$Q_{net\ down,SO} = \frac{V_{b,MO}}{3} - V_{f,SO} + Q^\circ_{net\ down,SO} \qquad (30)$$

Equations (28) and (30) show that for $v_{b,MO} = 0$, the net upflow relative to the stationary observer equals the upflow as though the interstitial liquid were frozen, minus the actual downflow relative to the moving observer. Also, it is convenient to note that for $v_{b,MO} = 0$, subscripts BO and MO become equivalent to each other.

$Q^\circ_{net\ down,SO}$ is a function of $M$ and $T$. This is shown in Figure 8. The function was obtained with the digital computer by numerically performing the double integration of Equation (29) for the various velocity profiles such as those of Figures 4, 5, and 6.

By extending this analysis further for $v_{b,MO} = 0$, $Q_{net\ up,SO}$ was separated into its upward moving portion $Q_{up,SO}$ and its downward moving portion $Q_{down,SO}$. This was carried out for various values of $T$. Figure 9 shows the numerically obtained results for $T = 0$. The dotted curve, which applies to hypothetical plug flow within each PB, was also derived analytically.

All of the foregoing analysis also applies to a stationary

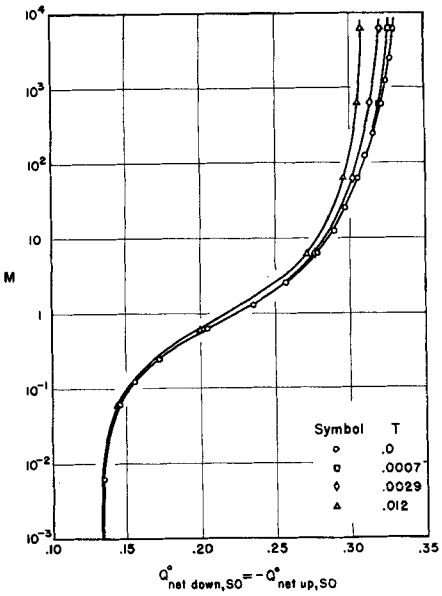


Fig. 8. Dimensionless relationship for flow through the foam as a whole.

foam; that is, where $v_{f,SO} = 0$, provided the rate of feed equals the rate of withdrawal from the bottom so as to maintain steady state.

In principle, the basic theory developed here should be extendible to foam draining at unsteady state, provided the rate of drainage is slow enough to allow a varying steady state velocity profile in a PB to be applied at unsteady state. A differential material balance over an incremental height of column would also be involved. However, the authors have not yet digressed along this particular avenue of investigation.

## FOAM DENSITY AND EXIT

An interesting consequence of the model is that the foam density should be substantially uniform along the column between any inlet or outlet stream and the inlet or outlet stream immediately above or below [which implies $dr_o/dz = 0$ in Equation (18)]. Thus, in Figure 1 for example, $\mathcal{D}$ should be uniform from the feed inlet on down to the surface of the liquid pool.

That this should be so can be seen by considering the foam densities at any two different levels in the bottom section of the column. By simple material balance, $q_{net\ down,SO}$ at the lower level must equal that at the higher level. If $\mathcal{D}$ were greater at the lower level than at the higher level, $A_{PB}$ would also have to be greater at the lower level since $A_{col}$ is fixed and $P$ would not change unless there were bubble coalescence. With a greater $A_{PB}$, the resistance to interstitial flow would be reduced. However, the driving force $g_{eff}$ would decrease only slightly because generally the dominant term by far in Equation (18) is $g_z$, which here is just $g$. Therefore, $v_{z,max,SO}$ would clearly be greater. [This may also be seen from Equations (6), (14), and (16) when combined with Figure 3.] Then, by substituting in the definition for $Q_{net\ down,SO}$ [which is analogous to Equation (22)], $Q_{net\ down,SO}$ would be smaller. Also, by substitution in Equation (25), $V_{f,SO}$ would also be smaller since $v_{f,SO}$ would increase only slightly. Substituting these results in Equation (30) would make $Q^{\circ}_{net\ down,SO}$ decrease, since $V_{b,MO} = 0$. From Figure 8, this in turn would mean a smaller $M$, which by Equation (16) would yield a smaller $r_o$. By the geometry of the PB, a smaller $r_o$ would mean a smaller $A_{PB}$ and a smaller $\mathcal{D}$. However, this contradicts the original trial assumption of a higher $\mathcal{D}$ at this lower level, and so is absurd.

By a similar line of reasoning, an initial assumption of a smaller $\mathcal{D}$ at the lower level also results in an absurdity. Hence $\mathcal{D}$ at the lower level must equal that at the higher level. In other words, the foam density is uniform in the bottom section of the column.

The foam density should also be uniform in the top section of the column (above the feed point) but, of course, at a lower value than that in the bottom section. As before, this is predicated on the absence of coalescence.

In order to determine actual values for the foam density at the top of the column and the rate of overhead takeoff, it is first necessary to consider the manner of takeoff. Let the takeoff be through a smooth bend of uniform cross section equal to that of the column $A_{col}$. Equating $v_{f,SO}$ to the maximum downward velocity (relative to MO) in a PB averaged for the various orientations, one gets $v_{z,max,MO} = (3/2)\ v_{f,SO}$ at the top of the column. This situation will be termed here *normal exit*.

Actually, the particular choice of criteria for normal exit is not critical. In fact, in the earlier stages of the present study, the authors considered $v_{z,max,MO} = v_{f,SO}$. That choice yielded results which were not very different from those obtained with $v_{z,max,MO} = (3/2)\ v_{f,SO}$.

Normal exit requires that the bulk foam rise up the column substantially in plug flow (which should not be confused with plug flow within a PB). With a uniform $A_{col}$ of more than several square centimeters this is essentially the case. However, obstructions in the column can cause sudden changes in $v_{f,SO}$, thus voiding the condition of normal exit.

The foam density at the top of the column can now be evaluated for normal exit by simultaneous trial and error solution of Figure 3 together with Equations (6), (8), (9), (12), (14), (16), (18), and (31):

$$v_{f,SO} = \frac{G}{A_{col}}\left(1 + \frac{V_L}{V_G}\right) \qquad (31)$$

Here, $v_{z,max}$ of Equation (14) is $v_{z,max,MO}$ which equals $(3/2)\ v_{f,SO}$ by virtue of normal exit. To simplify matters, Equation (18) usually can be approximated by $g_{eff} = g$. Also, $t = 0$ is usually satisfactory since the bubble films are very thin in the top section of the column.

After $D$ has been found by Equation (32) as discussed later, $W$ is obtained from Equation (1). By simple conservation of mass, $q_{net\ down,SO} = W$. Then the foam density in the lower section of the column, that is, below the feed point, can be evaluated by simultaneous trial and error solution of Figures 3 and 8 and Equations (6), (7), (8), (9), (12), (14), (16), (18), (25), (30), (31), and (22) with subscript net down replacing net up. With $dp_{out}/dz$ primarily

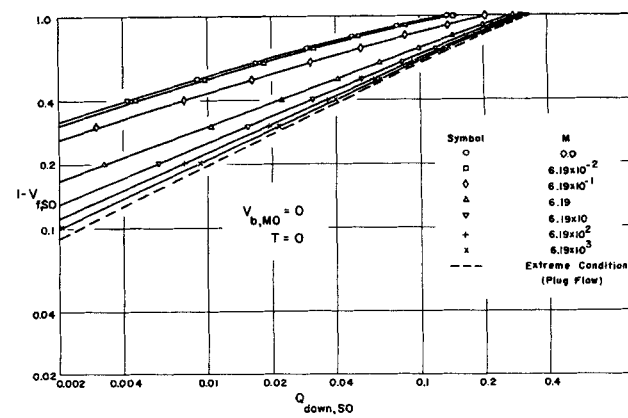


Fig. 9. Dimensionless relationship for exclusively downward flow through the foam as a whole.

due to the weight of the foam, Equation (18) can be well approximated by $g_{eff} = g\ (1 - \mathfrak{D})$. Provision should be made for $t$.

Surface viscosity $\mu_s$ for use in Equation (16) can be independently measured for the particular system by several methods (*8, 21*) including that employed in Part II of this paper. Alternatively, and perhaps more suitably for the present purpose, $\mu_s$ can be obtained by combining the theoretical relationships of the present part with a set of experimental results for the system in a properly operating foam column. This last method requires no concentration measurements and can be conveniently carried out with a rising or with a stationary foam. For the latter case, it might be added that since there is no overhead takeoff for a stationary foam, considerations relating to normal exit do not enter.

Approximate values of $\mu_s$ may also be found in standard references (*8, 21*) and other sources in the literature. For certain systems $\mu_s$ can vary markedly over narrow ranges of temperature.

Other physical properties can be obtained in the usual ways. For dilute solutions $\mu$ and $\rho$ are often nearly those of the solvent.

The rate of collapsed overhead takeoff equals $q_{\text{net up,SO}}$ at the top of the column. For normal exit, it is obtained with $v_{z,\max,\text{SO}} = (3/2)\ v_{f,\text{SO}}$, and $v_{b,\text{SO}} = 0$ by combining with Equations (7), (14), and (22) to give Equation (32):

$$D = 17.6(Q_{\text{net up,SO}}H_{eff})\frac{A_{col}\,v^2_{f,\text{SO}}}{h_{eff}\,d^2_{s1}\,(1 + V_L/V_G)} \quad (32)$$

The quantity $Q_{\text{net up,SO}}H_{eff}$ is a function of $\mu^2 v_{f,\text{SO}}/\mu_s^2 h_{eff}$, which can be shown with $t = 0$ by simultaneous solution of Equations (6), (14), (16), (17), and (28) together with Figures 3 and 8. Figure 10 shows this function. Substitution in Equation (32) then gives $D$.

If $t$ is known, $3tG/d_{s2}$ can be added to $D$ from Equation (32) to allow for the liquid carried out in the bubble faces. However, this is generally a very small contribution.

It should be noted that because of the velocity profiles within the PBs, $D/G \neq V_L/V_G$ at the top of the column. Rather, it can be shown from the foregoing that $1.25\ D/G < V_L/V_G < 2D/G$ at the top.

## APPLICATION TO DESIGN

In predicting the performance of a foam fractionation column of the type described earlier and represented in Figure 1, Equation (32) is the key.

First, $h_{eff}$ is obtained from Equation (12) with $g_{eff} = g$. Then, as a first trial, $\mathfrak{D}$ in the upper part of the column can be assumed to be small. Thus $V_L/V_G$ can be neglected, and $v_{f,\text{SO}}$ is obtained from Equation (31). Substitution gives the quantity $\mu^2 v_{f,\text{SO}}/\mu_s^2 h_{eff}$ from which the quantity $Q_{\text{net up,SO}}H_{eff}$ is read from Figure 10. Substitution in Equation (32) yields $D$.

For fairly dry foam, $D$ from the first trial can be accepted as is. For wetter foam, $V_L/V_G$ can be calculated (by the trial and error procedure for $\mathfrak{D}$ mentioned earlier) for use in a second trial. However, a quick approximation to the correction that would result is simply to multiply $D$ by the quantity $(1 + 3D/G)$.

This correction factor is arrived at by taking $V_L/V_G$ as approximately $1.6D/G$ and then by considering the various effects of $V_L/V_G$, namely on $v_{f,\text{SO}}$ via Equation (31), on $h_{eff}$ via Equation (18) with $\frac{dp_{out}}{\rho dz} = \frac{1.6Dg}{G}$, on the middle region of Figure 10, and finally on $D$ itself via Equation (32). The correction is usually modest. Any contribution to $dp_{out}/dz$ occasioned by frictional resistance

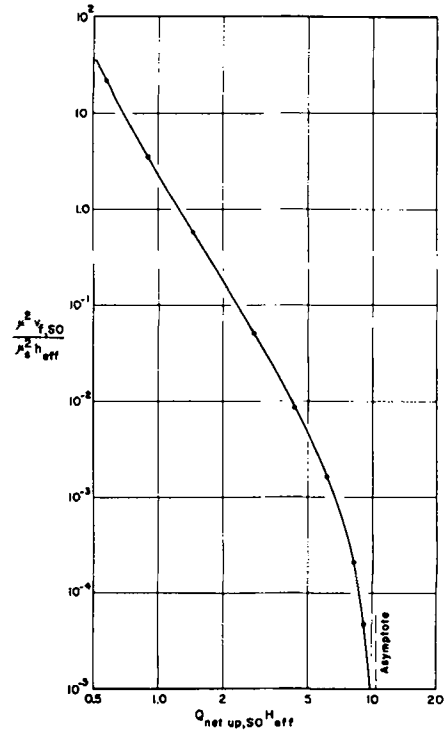


Fig. 10. Relation for $Q_{\text{net up, SO}}H_{\text{eff}}$ in the top section of a foam column. Asymptote of 10.6 shown for $\mu_S = \infty$ or $v_{f,\text{SO}} = 0$.

to the bulk movement of the foam is neglected here. The small amount of liquid in the bubble faces is also neglected.

[The surface viscosity for use in Figure 10 can be obtained as described earlier. If a determination by flow through a stationary foam is selected, it is advisable to conduct the experiment before the foam grows too old. Otherwise, the larger bubbles in the foam will grow at the expense of the smaller bubbles because of the slight difference in pressure which causes gas to diffuse across the films. In some cases, appreciable changes in bubble size distribution can be observed in less than an hour. In such cases, the new distribution of bubble diameters must be employed.

For fairly rigid PB walls, as is often the case in foams of protein origin (*8*), precision in the determination of the high surface viscosity is not necessary. This is evident from Figure 10 wherein the curve approaches an asymptote. In fact, simply setting $\mu_s = \infty$ may be quite satisfactory in such cases. However, this simplification is not advisable for detergent foams because their PB walls are generally far from rigid (*8*).]

Corrected $D$ is subtracted from $F$ by Equation (1) to yield $W$.

With the feed point sufficiently far above the liquid pool so that $C_L$ may be taken as equal to $C_F$, Equations (1) and (3) can be combined to give $C_W = C_F - \frac{6G\Gamma}{Wd_{s2}}$. Substitution yields $C_W$. Then, substitution in Equation (2) yields $C_D$. Since the diameter is that for the bubbles as spheres in the liquid pool, strictly speaking the constant 6 should be replaced by 6.59 to account for their distortion to regular dodecahedra in the foam.

If column operation is altered so that the feed enters the liquid pool directly, $C_L$ in Equation (3) should be replaced by $C_W$. Combination with Equation (1) yields $C_W = C_F - \frac{6G\Gamma}{Fd_{s2}}$. The replacement of 6 by 6.59 should not apply to this last equation. The bubbles distort only after they have left the liquid pool. Thus the incremental

adsorption due to distortion is only gained at the expense of solute in interstitial liquid which is not replaced by any rinsing feed.

Prediction of performance is sensitive to bubble size. If the size is not uniform, the distribution must be known with some accuracy. Then $d_{31}$ and $d_{32}$ should be calculated from Equation (33) which is general for $d_{ek}$:

$$d_{ek}^{e-k} = \frac{\sum_i n_i d_i^e}{\sum_i n_i d_i^k} \tag{33}$$

Column height does not enter into the calculation of $D$. Indeed, except for insuring $C_L = C_F$ for side feeding, it is not involved at all. Thus, making the column still taller should not affect $C_D$. However, it must be remembered that the analysis is based on the absence of bubble coalescence in the column. Actually, increasing the height increases the residence time of the foam and so could promote coalescence. For the same reason, so could decreasing the gas rate. Coalescence would decrease $D$ and increase $C_L$ through internal reflux, thus increasing $C_D$. If such be the case it is recommended that $d_{31}$ be taken at the top of the column. To estimate how $d_{ek}$ is altered by moderate coalescence, it may be approximated from a known $d_{ek}$ in the same section* of the column with the relationship $\frac{d_{ek,2}}{d_{ek,1}} = \left(\frac{\mathcal{D}_1}{\mathcal{D}_2}\right)^{1/2}$ if the value of $\mathcal{D}_1/\mathcal{D}_2$ is available from measurement or some other source.

The method can also be applied to calculate takeoff rates from columns with external reflux. For such columns, Equation (32) is applied to the section above the reflux inlet.

By material balance, the recyclic nature of external reflux does not allow equality between $C_R$ and $C_L$ at steady state conditions lest the already high $C_R$ build up to an impossible value. Thus, with external reflux, increasing the column height can be of importance by allowing for increased contact between downcoming reflux and rising foam.

The extent of enrichment in a finite refluxing column depends in part on the mass transfer coefficient and the magnitudes of the counter-flowing streams. These latter can be estimated by means of the present model. Such calculations show substantial internal recycle within the column.

In a previous investigation (5) a relationship between exit concentrations was developed for a refluxing column which is long enough to allow the concentration in the downflowing interstitial liquid at some level in the column to approach the concentration of the upflowing interstitial liquid at that level, provided the feed point is in the liquid pool. Equation (34) is an equivalent form of that relationship:

$$C_D = C_W + \frac{6G\Gamma}{D'd_{32}} \tag{34}$$

If the feed point is well above the liquid pool so that an effective stripping section is included in the column, Equation (34) can be modified to Equation (35):

$$C_D = C_F + \frac{6G\Gamma}{D'd_{32}} \tag{35}$$

To allow for the small incremental adsorption associated with dodecahedral distortion, the constant 6 in Equation (34) may be replaced by the quantity $\left(6.59 - \frac{0.59}{R+1}\right)$. In Equation (35), the constant 6 should be replaced by just 6.59.

Since $D' = D/(R+1)$, Equation (34) or (35) can be combined with Equation (32) and appropriate overall balances to yield concentrations and flow rates for the exit streams from the column. The general method is thus readily extended to include long refluxing enriching columns and long combined columns.

* Meaning not separated by an inlet or outlet stream.

## SUMMARY

A new model to describe the interstitial flow and drainage in a stationary or moving foam of noncoalescing bubbles was proposed and developed for steady state conditions. It involved solving the differential momentum conservation equation for flow through a representative capillary (or Plateau border) of curved triangular cross section with nonrigid boundaries characterized by a Newtonian surface viscosity. A finite difference approach was employed with a digital computer to obtain the velocity profiles. These, in turn, were combined by digital computation with a velocity component balance accounting for the random orientation of capillaries and the upward movement (if any) of the bulk foam.

Results were obtained in generalized dimensionless form so as to enable prediction of foam densities and flow rates for a wide range of conditions. When combined with material balances and considerations relating to surface adsorption, surfactant concentrations and rates of flow for the exit streams from a foam fractionation column can be estimated. A procedure for carrying out this estimation is outlined, and an extension to coalescing foams is suggested.

Results of the theory have been confirmed by experiment. Details of this confirmation are presented in Part II.

## LITERATURE CITED

1. Adamson, A. W., "Physical Chemistry of Surfaces," Interscience, New York (1960).
2. Bikerman, J. J., "Foams: Theory and Industrial Applications," Reinhold, New York (1953).
3. Bird, R. B., W. E. Stewart, and E. N. Lightfoot, "Transport Phenomena," Wiley, New York (1960).
4. Brady, A. P., and S. Ross, *J. Am. Chem. Soc.*, **66**, 1348 (1944).
5. Brunner, C. A., and R. Lemlich, *Ind. Eng. Chem. Fundamentals*, **2**, 297 (1963).
6. *Chem. Eng.*, **68**, No. 7, p. 100 (1961).
7. Corkill, J. M., J. F. Goodman, C. P. Ogden, and J. R. Tate, *Proc. Roy. Soc. (London)*, Ser. **A273**, 84 (1963).
8. Davies, J. T., and E. K. Rideal, "Interfacial Phenomena," Academic Press, New York (1961).
9. Gibbs, J. W., "Collected Works," Vol. 1, Longmans Green, New York (1928).
10. Haas, P. A., and H. F. Johnson, "A Model and Experimental Results for Drainage of Solution between Foam Bubbles," presented at Am. Chem. Soc. national meeting, Chicago, Illinois (Aug. 30 to Sept. 4, 1964).
11. Harper, D. O., and R. Lemlich, *Ind. Eng. Chem., Process Design and Devel. Quarterly*, **4**, 3 (1965).
12. Hildebrand, F. B., "Introduction to Numerical Analysis," McGraw-Hill, New York (1956).
13. Husmann, W., *Textil-Rundschau*, **17**, 88 (1962).
14. Jacobi, W. M., K. E. Woodcock, and C. S. Grove, Jr., *Ind. Eng. Chem.*, **48**, 2046 (1956).
15. Klein, S. A., and P. H. McGauhey, *Journal W.P.C.F.*, **35**, 100 (1963).
16. Lemlich, R., and E. Lavi, *Science*, **134**, No. 3473, p. 191 (1961).
17. Leonard, R. A., Ph.D. dissertation, University of Cincinnati, Cincinnati, Ohio (June, 1964).
18. ———, and R. Lemlich, *Chem. Eng. Sci.*, to be published.
19. Manegold, E., "Schaum," Strassenbau, Chemie und Technik Verlagsgesellschaft m.b.H., Heidelberg (1953).

20. Miles, G. D., L. Shedlovsky, and J. Ross, *J. Phys. Chem.*, 49, 93 (1945).
21. Mysels, K. J., K. Shinoda, and S. Frankel, "Soap Films, Studies of their Thinning and a Bibliography," Pergamon Press, New York (1959).
22. Osipow, L. I., "Surface Chemistry, Theory and Industrial Applications," ACS Monograph Series 153, Reinhold, New York (1962).
23. Ross, S., *J. Phys. Chem.*, 47, 266 (1943).
24. Rubin, E., and E. L. Gaden, Jr., "New Chemical Engineering Separation Techniques," Chap. 5, H. M. Schoen, ed., Interscience, New York (1962).
25. Schnepf, R. W., and E. L. Gaden, Jr., *J. Biochem. Microbiol. Tech. Eng.*, 1, 1 (1959).
26. ———, E. Y. Mirocznik, and E. Schonfeld, *Chem. Eng. Progr.*, 55, No. 5, p. 42 (1959).

*Manuscript received March 23, 1964; revision received August 14, 1964; paper accepted September 9, 1964.*

# Part II. Experimental Verification and Observations

**Experimental results obtained over a wide range of variables from three different foam fractionation columns support the theory developed in Part I.**

In Part I a theory was developed for interstitial flow in foam which could be applied to foam fractionation. This paper presents the results of experimental tests of this theory.

## EXPERIMENTAL

A foam fractionation column of 4.1-cm. I.D. was constructed of glass as shown in Figure 1. Thoroughly humidified nitrogen was bubbled up through the liquid pool at the bottom, forming foam which rose up the column and passed out through the horiontal line of 0.8-cm. I.D. at the top. The liquid level of the pool at the bottom of the column was maintained approximately 80 cm. below the overhead foam line. The feed point and pressure probe were adjustable up and down the column. Operation was at 25° ± 1°C. in a temperature-controlled room. Further details of experiments and results have been placed on file (*6*).

A bubbler with a single orifice was employed in order to obtain a uniform bubble size for a given run. The frequency at which bubbles were formed was measured with a stroboscopic light. The bubble diameter was then calculated by $d_{30} = \sqrt[3]{6G/\pi N}$. The feed was a $5 \times 10^{-4}$ molar aqueous solution of the surfactant Triton X-100, which can be considered to have the formula $C_8H_{17}—\phi—(OCH_2CH_2)_{9.7}—OH$.

After a foam with bubbles of uniform size and known diameter had been formed, the gas flow to the bubbler was usually stopped. The liquid feed rate through the foam was continued for a while to achieve steady state conditions and to allow the flow rate to be checked. Then the feed line was closed and the bottom exit was blocked so that the volume of interstitial liquid in the foam could be measured when the foam collapsed. During these latter operations, the faces of the foam bubbles were observed in order to obtain a measure of their thickness by their progressive color changes with a technique (*1*, *7*) based on the diffraction of incident light.

Two runs were made at continuous gas flow conditions. These required a much longer time to reach steady state and still longer to collect enough overhead foam for a measurement of collapsed volume. Furthermore, it was difficult to maintain the relatively dry foam in the necking section at the top of the column. The strain of the tenfold reduction in cross section would often suddenly collapse all the foam in the entire top section of the column, thus invalidating the run. Accordingly, most of the runs were not of this type involving continuous gas flow, since much of the information that could be obtained from this column could be gained just as well and more quickly by simply letting liquid flow down through stationary foam, that is with $v_{f,\,so} = 0$.

Surface tension was measured with a ring tensiometer yielding values close to those obtained by others (*2*, *4*). Viscosity was measured with an Ostwald viscosimeter, yielding values close to those of pure water. $\Gamma$ determined from surface tension via Gibbs' equation generally compared favorably with that determined from Equations* (2) and (3) from experiments with the foam column. Both methods yielded $\Gamma$ of about $2.8 \times 10^{-10}$ g. moles/sq.cm., except for very dry foams in which a micelle double film (*5*) may have formed. Solute concentrations were measured by ultraviolet spectrophotometry.

## RESULTS

For each run, the experimental values for $V_L/V_G$, $t$, and $d_{32} = d_{31} = d_{30}$ were substituted in Equation (8) to give $A_{PB}$. This was for the section of column from the feed point down to the surface of the liquid pool. Substitution in Equation (6) gave $r_o$. $T$ followed from Equation (17).

Measurements with the pressure probe showed that the entire weight of foam was transmitted as hydrostatic head. Observation of face colors showed no variation of $t$ with height, which implies $dr_o/dz = 0$ and also a uniform foam density. This uniformity in $\mathfrak{D}$ accords with the prediction

* All equation numbers refer to Part I.